Charging mechanism in a SiO_2 matrix embedded with Si nanocrystals

Y. Liu, T. P. Chen,[a] and L. Ding
School of Electrical and Electronic Engineering, Nanyang Technological University, Singapore 639798, Singapore

S. Zhang and Y. Q. Fu
School of Mechanical and Aerospace Engineering, Nanyang Technological University, Singapore 639798, Singapore

S. Fung
Department of Physics, The University of Hong Kong, Hong Kong

(Received 15 May 2006; accepted 1 September 2006; published online 13 November 2006)

One of the applications of a Si nanocrystals (nc-Si) embedded in a SiO_2 matrix is in the area of nonvolatile memory devices based on the charge storage in the material system. However, whether the charge trapping mainly occurs at the nc-Si/SiO_2 interface or in the nc-Si is still unclear. In this work, by x-ray photoemission spectroscopy analysis of the Si 2*p* peaks, the concentrations of both the nc-Si and the Si suboxides that exist at the nc-Si/SiO_2 interface are determined as a function of thermal annealing, and the charging effect is also measured by monitoring the shift of the surface C 1*s* peak. It is observed that the annealing-caused reduction of the total concentration of the interfacial suboxides is much faster than that of both the C 1*s* shift and the nc-Si concentration. In addition, the trend of the C 1*s* shift coincides with that of the nc-Si concentration. The results suggest that the Si nanocrystal, rather than the nc-Si/SiO_2 interface, plays the dominant role in the charging effect. © *2006 American Institute of Physics*. [DOI: 10.1063/1.2374929]

Si nanocrystals (nc-Si) embedded in SiO_2 films have potential applications in nonvolatile memory devices.[1–8] For the nonvolatile memory application, the nc-Si is normally confined in a narrow layer in the gate dielectric near the substrate. Charging /discharging the nc-Si leads to the flatband voltage shifts, yielding two distinguishable memory states. There have been many studies on the nc-Si nonvolatile memory devices. However, there are few experimental studies so far on the charging mechanism of the nc-Si/SiO_2 system. It is still in doubt whether the charging mainly occurs at the nc-Si/SiO_2 interface or inside the nc-Si. In this work, an x-ray photoelectron spectroscopy (XPS) experiment is carried out on the system of nc-Si embedded in SiO_2 thin films synthesized by Si ion implantation followed by thermal annealing. The C 1*s* core level on the sample surface due to contamination is used to monitor the charging effect, while the Si 2*p* peaks are analyzed to obtain the information of the concentrations of the nc-Si (Si^0) and the Si suboxides (Si^{1+}, Si^{2+}, and Si^{3+}) that exist at the nc-Si/SiO_2 interface. By examining the changes of the charging effect and the concentrations of the nc-Si and the Si suboxides with thermal annealing, one may be able to answer the question whether the nc-Si or the nc-Si/SiO_2 interface plays a dominant role in the charging effect.

SiO_2 thin films of 30 nm in thickness were grown on *p*-type Si wafers with (100) orientation by thermal oxidation in dry oxygen at 950 °C. Then Si ions were implanted into the SiO_2 films with the dose of 8×10^{16} cm^{-2} at 1 keV. Thermal annealing was carried out in N_2 ambient. For the experiment of annealing temperature, the temperature was varied from 700 to 1100 °C but the annealing time was fixed at 20 min; for the experiment of annealing time, the time was varied from 0 to 100 min, while the annealing temperature was kept at 1000 °C. The XPS experiment was performed by using a Kratos Axis spectrometer with monochromatic Al $K\alpha$ (1486.71 eV) x-ray radiation. Si 2*p* spectra were taken to study the changes in the concentrations of five Si oxidation states. C 1*s* spectra due to the surface carbon contamination were also rerecorded to monitor the x-ray-induced charging effect in the samples.

It has been known that x-ray irradiation can cause charging in both SiO_2/Si system[9] and nc-Si/SiO_2 system.[10,11] For the system of nc-Si embedded in a SiO_2 matrix, photoemission may leave positive charges in the nc-Si and SiO_2 as well as at the nc-Si/SiO_2 interface, leading to a core level shift to a higher binding energy. The C 1*s* core level shift shown in Fig. 1 is an indicator of the charging effect. The C 1*s* core level on pure SiO_2 surface has a shift of ~0.8 eV relative to the C 1*s* reference, while it shows shifts of ~2.1 and ~1.6 eV for the as-implanted sample and the sample annealed at 1100 °C for 20 min, respectively. This indicates that the charging effect is greatly enhanced by the introduction of the nc-Si into the SiO_2 matrix. The reduction of the charging effect of the annealed sample is mainly attributed to the reduction of the nc-Si concentration due to the surface oxidation, as discussed later.

Figures 2(a) and 2(b) show the XPS Si 2*p* core level peaks for the as-implanted and the sample annealed at 1100 °C for 20 min, respectively. Five oxidation states Si^{n+} ($n=0-4$) could exist in the Si-implanted SiO_2 films.[10,11] Here Si^0 and Si^{4+} correspond to the nc-Si and SiO_2, respectively, while Si^{n+} ($n=1-3$) correspond to the Si suboxides

[a]Electronic mail: echentp@ntu.edu.sg

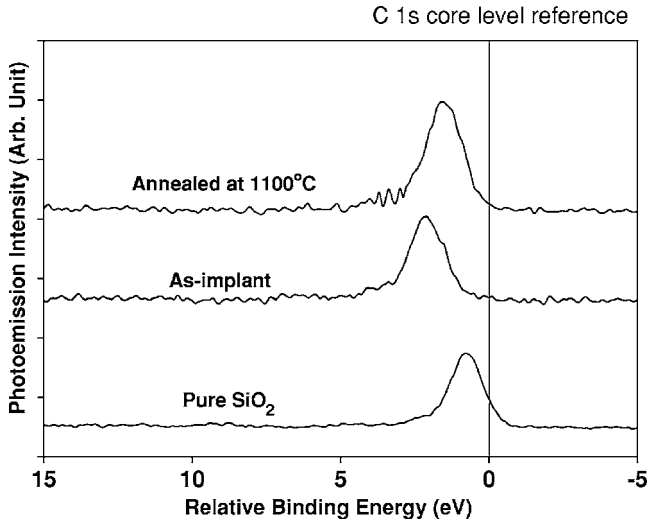

FIG. 1. C 1*s* core level shift relative to the reference for the pure SiO_2 sample, the as-implanted sample, and the sample annealed at 1100 °C for 20 min.

(Si_2O, SiO, and Si_2O_3) which exist at the nc-Si/SiO_2 interface. A curve fitting to the Si 2*p* core level peaks is carried out by decomposing the spectrum into the Si $2p_{1/2}$ and $2p_{3/2}$ partner lines for the five oxidization states. The spin-orbit splitting is fixed at 0.6 eV, and the Si $2p_{1/2}$ and $2p_{3/2}$ intensity ratio is set to $\frac{1}{2}$ for all of the five oxidation states.[12] Only the sum of the Si $2p_{1/2}$ and $2p_{3/2}$ partner lines is shown in Fig. 2 for a clear presentation. As can be observed in Fig. 2, the peak areas of the five oxidation states change with annealing, showing that the concentrations of the five oxidation states vary with the annealing. The relative concentration of each oxidation state can be obtained by calculating the ratio of $I_{Si^{n+}}/I_{total}(n=0-4)$, where $I_{Si^{n+}}$ is the peak area of the oxidation state Si^{n+} and I_{total} is the total area $(=\Sigma_{i=0}^{4} I_{Si^{n+}})$ of the Si 2*p* peaks. It can be observed from Fig. 2 that after the annealing at 1100 °C for 20 min, the SiO_2 (Si^{4+}) concentration increases, while the concentrations of both the Si suboxides (Si^{1+}, Si^{2+}, and Si^{3+}) at the interface and the nc-Si (Si^0) decrease. The reduction of the suboxides is due to the thermal decomposition of the suboxides. The thermal decomposition during the annealing is to form stoichiometric SiO_2 and Si nanocrystals.[10] In other words, the thermal decompositions lead to the growth of both SiO_2 and the nc-Si. However, although the annealing was carried out in nitrogen gas with purity better than 99.99%, there is some residual oxygen presented in the furnace, and some of the nc-Si is oxidized during the annealing. Therefore, the Si^0 concentration decreases, while the Si^{4+} concentration increases after the annealing.

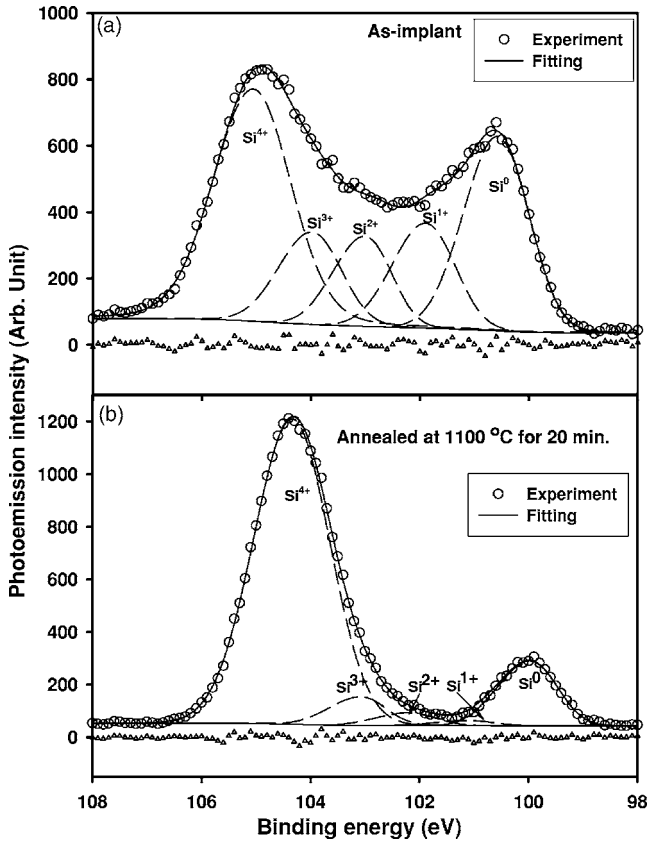

FIG. 2. The deconvolution of Si 2*p* spectra for the as-implanted sample (a) and the sample annealed at 1100 °C for 20 min (b). The unfilled triangles represent the difference between the measurement and the fitting.

Figures 3(a)–3(c) show the C 1*s* shift, the total concentration $(\Sigma_{i=1}^{3} I_{Si}/I_{total})$ of the interfacial suboxides, and the nc-Si concentration as a function of the annealing temperature, respectively. The annealing time is fixed at 20 min. The C 1*s* shift decreases with annealing temperature, showing that the charging effect is reduced by annealing. However, it should be noted that the reduction of the charging effect is not drastic. For example, the C 1*s* shift decreases from ~2.1 eV of the as-implanted sample to ~1.6 eV of the sample annealed at 1100 °C for 20 min. The shift of 1.6 eV is still much larger than that (0.8 eV) of the pure SiO_2 sample, indicating that the system of nc-Si embedded in SiO_2 maintains a good charge storage capability. The total concentration of the interfacial suboxides and the nc-Si concentration both decrease with annealing temperature, as shown in Figs. 3(b) and 3(c), respectively. The decrease of the total concentration of the interfacial suboxides is attributed to the thermal decomposition of the suboxides, and the decrease of the nc-Si concentration is due to the oxidation of the nanocrystal by the residual oxygen during the annealing, as pointed out earlier. From a comparison among the annealing-temperature effects on the C 1*s* shift [Fig. 3(a)], the total concentration of the interfacial suboxides [Fig. 3(b)], and the nc-Si concentration [Fig. 3(c)], one may conclude that the nc-Si plays a more important role in the charging effect than the nc-Si/SiO_2 interface. For example, with a reference to the as-implanted sample, the annealing at 700 °C causes relative reductions (in percentage) of ~10% in the C 1*s* shift, ~25% in the nc-Si concentration, and ~55% in the total concentration of the interfacial suboxides. The reduction of the total concentration of the interfacial suboxides is much faster than that of both the C 1*s* shift and the nc-Si concentration, suggesting that the interface would not play a dominant role in the charging effect.

The conclusion that the nc-Si plays a more important role in the charging effect than the nc-Si/SiO_2 interface is further supported by the experiment of annealing time, as shown in Fig. 4. The experiment was carried out at a fixed temperature of 1000 °C. As shown in Fig. 4(a), the total

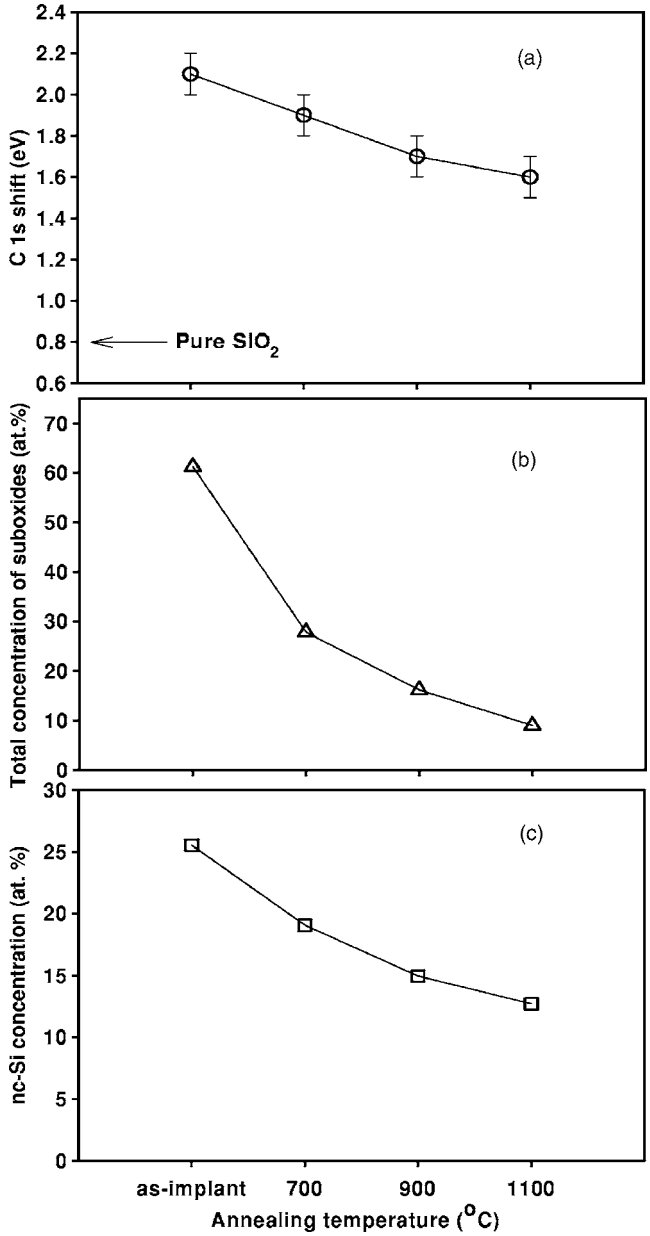

FIG. 3. Annealing-temperature effect on the C 1*s* core level shift (a), the total concentration of the interfacial suboxides (b), and the nc-Si concentration (c). The annealing duration is fixed at 20 min.

concentration of the interfacial suboxides is drastically reduced from ~60% for the as-implanted sample to ~10% after the annealing for 20 min and remains unchanged for prolonged annealing. However, as shown in Fig. 4(b), the C 1*s* shift is gently reduced from ~2.1 eV for the as-implanted sample to ~1.6 eV after the annealing for 20 min and remains at ~1.8 eV for prolonged annealing. Most importantly, the trend of the C 1*s* shift with annealing time coincides with that of the nc-Si concentration with annealing time, as shown in Fig. 4(b). This strongly suggests that the nc-Si plays a key role in the charging effect.

In summary, the experiments of annealing effects on the C 1*s* shift, the total concentration of the interfacial suboxides, and the nc-Si concentration have been carried out. It is observed that the annealing-caused reduction of the total concentration of the interfacial suboxides is much faster than

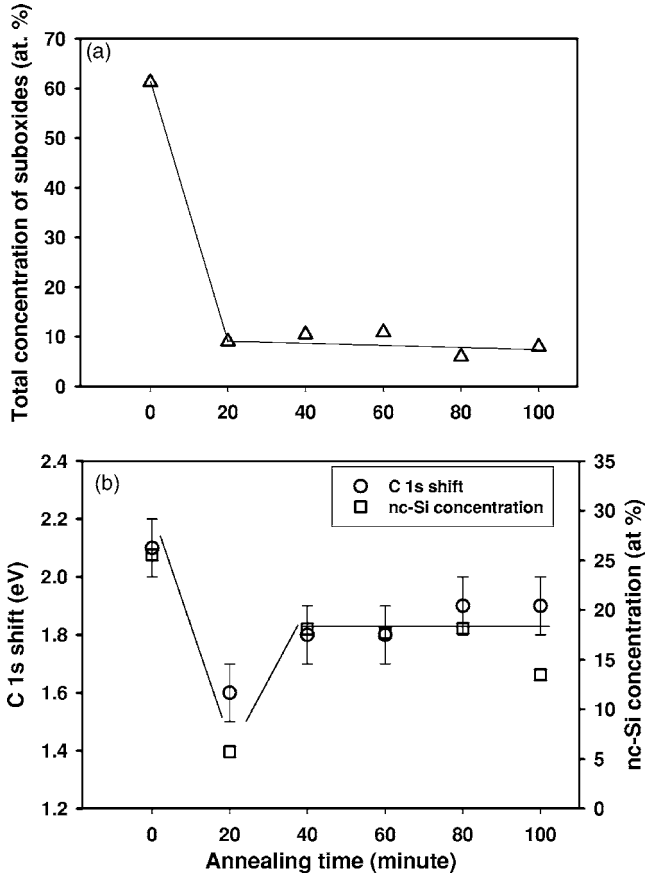

FIG. 4. (a) The total concentration of the interfacial suboxides as a function of annealing time; (b) the comparison between the nc-Si concentration and the C 1*s* core level shift as a function of annealing time. The annealing temperature is fixed at 1000 °C.

that of both the C 1*s* shift and the nc-Si concentration. In addition, the trend of the C 1*s* shift with annealing time coincides with that of the nc-Si concentration with annealing time. The results suggest that the nc-Si rather than the nc-Si/SiO_2 interface plays the dominant role in the charging effect in the system of nc-Si embedded in SiO_2.

This work has been financially supported by the Academic Research Fund of the Ministry of Education of Singapore under Project No. RG 1/04.

[1]S. Tiwari, F. Rana, H. Hanafi, A. Hartstein, E. F. Crabbé, and K. Chan, Appl. Phys. Lett. **68**, 1377 (1996).
[2]S. Tiwari, F. Rana, K. Chan, L. Shi, and H. Hanafi, Appl. Phys. Lett. **69**, 1232 (1996).
[3]R. A. Rao *et al.*, Solid-State Electron. **48**, 1463 (2004).
[4]P. Dimitrakis *et al.*, Solid-State Electron. **48**, 1511 (2004).
[5]J. Carreras, B. Garrido, and J. R. Morante, Microelectron. Reliab. **45**, 899 (2005).
[6]R. Ohba, N. Sugiyama, J. Koga, K. Uchida, and A. Toriumi, Jpn. J. Appl. Phys., Part 1 **39**, 989 (2000).
[7]C. Y. Ng, T. P. Chen, M. Yang, J. B. Yang, L. Ding, C. M. Li, A. Du, and A. Trigg, IEEE Trans. Electron Devices **53**, 663 (2006).
[8]C. Y. Ng, T. P. Chen, L. Ding, and S. Fung, IEEE Electron Device Lett. **27**, 231 (2006).
[9]S. Iwata and A. Ishizaka, J. Appl. Phys. **79**, 6653 (1996).
[10]Y. Liu, Y. Q. Fu, T. P. Chen, M. S. Tse, S. Fung, J. H. Hsieh, and X. H. Yang, Jpn. J. Appl. Phys., Part 2 **42**, L1394 (2003).
[11]T. P. Chen, Y. Liu, C. Q. Sun, M. S. Tse, J. H. Hsieh, Y. Q. Fu, Y. C. Liu, and S. Fung, J. Phys. Chem. B **108**, 16609 (2004).
[12]F. J. Himpsel, F. R. McFeely, A. Taleb-Ibrahimi, J. A. Yarmoff, and G. Hollinger, Phys. Rev. B **38**, 6084 (1988).